Use of Agricultural Waste to Prepare Modified an Activated Carbon (ACPO) for Removal Citric Acid from Aqueous Solutions

Aya Taha Shuib[1] , Muthana Muhammed Sirhan[2]

[1,2] Department of Chemistry, College of Education for Pure Sciences, University of Anbar, Ramadi, Iraq.

[1] E-mail: aya24u4008@uoanbar.edu.iq
[2] E-mail: muth_1974na@uoanbar.edu.iq

Abstract:

In this work, an adsorbent material was prepared from agricultural waste and used to remove citric acid from aqueous solutions. Pomegranate peels were chosen due to their chemical composition, which is rich in organic compounds with strong binding properties (such as gallic acid, ellagic acid, hydroxycinnamic acids, and flavone derivatives). The modified activated carbon (ACPO) was prepared from pomegranate peels through a carbonization process using sulfuric acid for 24 hours, followed by burning at 300°C for 3 hours, and then treated with a 35% H_2O_2 solution to increase porosity. The prepared material was characterized using XRD, FESEM, and EDX to determine the crystalline structure, surface morphology, and elemental composition, respectively. XRD results revealed the semi-crystalline nature of the activated carbon, while FESEM images showed a significant improvement in the pore network, and EDX analysis confirmed the presence of the main elemental components of the material.

The modified Activated carbon (ACPO) was selected as an adsorbent material for the removal of citric acid from aqueous solutions, with an evaluation of the effects of initial concentration, temperature, adsorbent dose, and contact time on adsorption efficiency. It was found that the highest removal efficiency was 98% when the adsorbent dose was 1 g. The application of Langmuir and Freundlich models showed good agreement with the experimental observations. The estimated thermodynamic data (ΔH = -30.6 KJ/mol, ΔS = -91.4 KJ/mol, and ΔG) indicate that the adsorption process of citric acid is exothermic and decreases with increasing temperature. The process was found to be spontaneous and accompanied by a decrease in entropy, indicating increased order on the surface of the adsorbent compared to the solution.

1.Introduction

Environmental pollution with hazardous organic substances is considered one of the most important issues worldwide due to its impact on human safety and ecosystems.[1] The presence of organic pollutants in the environment is particularly concerning because they affect the hormonal balance in humans as well as in wildlife. Carcinogenic chemicals are spread throughout the environment, including soil, air, groundwater, and surface water. Due to their continuous release into the environment, even in small amounts, they are classified as persistent substances.[2] Organic pollutants often undergo an oxidation reaction that leads to the formation of final products of carboxylic acids.[3] One of the most dangerous organic substances that can pose a risk to human health and dissolve very quickly in water is carboxylic acids.[4]. One of the main methods for addressing the problem of pollution is adsorption technology, because its cost is relatively low. Adsorption can be defined as the interaction between three components: the solvent, the adsorbent materials, and the adsorbed substance, which occurs on the surface.

The affinity of the adsorbed substance towards the adsorbent and its solubility in the solvent act as an interactive force that governs this adsorption.[5]Natural resources such as zeolite, organic aggregates, carbon, clay, and agricultural waste can be used as adsorption surfaces, in addition to using waste and nano oxides [6]

Activated carbon also known as activated charcoal is a highly porous and extensively processed form of carbon, characterized by its significantly large surface area, microcrystalline, non-graphitic, and amorphous structure, resulting in a network of interconnected pores[7], [8]There are two ways to activate carbon: chemically (using a chemical substance) or physically (thermal decomposition). Chemical activation is preferred over physical activation because it requires lower temperatures and a shorter time period.[9]Activated carbon has many physical and chemical properties. Chemical properties such as pH, ash content, and electrical conductivity, along with the physical properties of activated carbon, such as surface area and bulk density, play crucial roles in determining its suitability and fitness for specific purposes. These chemical and physical properties determine the appropriateness, and applications of activated carbon in various industries. Understanding these properties is essential for selecting the right type of activated carbon to meet specific purification or adsorption requirements.[10]Activated carbon can be used to remove of organic and inorganic pollutants, and its effectiveness in removing target molecules can be enhanced through adsorption by introducing specific functional groups onto the surface of the adsorbent material.[11] Activated carbon (AC) is widely used in various sectors, including industry, energy, healthcare, environmental protection, as well as for household purposes.[12] modification, and separating of diverse compounds in both gas and liquid forms[13] The use of carbon dates back to ancient times. In ancient Egyptian civilization, around 1500 BC, charcoal was used as an absorbent medicinal substance and as a purifying agent. It was used to remove color from aqueous solutions in 1786, which represents the first practical measurement of the adsorption power of charcoal in the liquid phase.[14] However, the concept of 'activation' as we understand it today began to take shape in the eighteenth century. In 1822 bussy introduced the first activated charcoal produced using a combination of physical and chemical activation by heating blood with potash. This type of charcoal was proven to be more effective compared to traditional burned charcoal.[15] Commercially marketable activated charcoal emerged thanks to the contributions of the Swedish scientist von Ostreiko, who patented this innovation in 1900 and 1901.[14] Despite the widespread use of activated charcoal, its high cost makes it not easily accessible to everyone. Additionally, the lack of inexpensive, high-quality materials that meet consumers' needs is an obstacle that hinders its wider spread.[16] In addition, the use of imported activated charcoal may have negative environmental impacts due to emissions resulting from the transportation process.[17] Recently, the production of activated carbon from agricultural waste has received increasing attention, such as rice husks.[18] , Pistachio shells[19] ,potato peels[20] ,cinnamon waste[12] , castor seed hull[21] , Carica Papaya Trunk[22] , date stone[23] , coconut fiber[24] , guinea corn husk[25] , Palm kernel shell and cake[26].

Huge amounts of waste are wasted annually around the world, reaching more than half a billion tons of vegetable and fruit residues. These wastes are likely to increase the emission of harmful gases that affect the environment and contribute to climate change if not managed properly. The problem worsens due to improper disposal methods, such as burying and burning in landfills, which lead to the leakage of these gases, especially methane, into the atmosphere. Therefore, there is an urgent need to find alternative ways to utilize agricultural waste, including converting it into useful absorbent materials[27].

Agricultural waste is considered a natural, economical, and environmentally friendly

adsorbent that helps in removing pollutants from wastewater. It can be extremely effective as a bio-adsorbent for removing contaminants, among which are pomegranate peels. Pomegranate is one of the most famous fruits in the world due to its delicious taste and high nutritional benefits. The peel accounts for about 30% of the fruit's weight, yet it is usually discarded as waste. These peels contain two main hydroxybenzoic acids, gallic acid and ellagic acid, in addition to hydroxycinnamic acids and flavonoid derivatives. Pomegranate peels are also considered a cheap and highly effective bio-adsorbent, allowing for environmentally friendly pollutant absorption and possessing a high capacity for absorbing organic pollutants, dyes, and metals, with minimal environmental impact[28].

2. Materials and methods

2.1. Chemicals:

Citric acid (99%), Sodium hydroxide (Qualikems), pomegranate peels were collected from local market, distilled water, phenol naphthalene reagent, H_2O_2, H_2SO4, Na_2CO_3, magnetic stirrer, electric grinder (Germany), drying oven (Sanyo - Japan), conical flask, pipette, 53 µm sieve (China), 150 µm sieve (China) ,FTIR (Bruker-Germany).

2.2.1. Preparation of the Adsorbent (ACP)

Pomegranate peels were ground using an electric grinder after being dried for two weeks under sunlight. Then, 20 g of the peels were taken after sieving them through a 150 µm sieve. Afterwards, these peels were converted into charcoal using concentrated sulfuric acid (H_2SO_4) at 50°C with the addition of 5 mL of water for 24 hrs. The mixture was then transferred to a crucible covered will Aluminum foil and heated at 300°C for 3 hrs. then left to cool for 24 hrs. Subsequently, the resulting charcoal was washed three times with distilled water to remove the acid, followed by washing three times with (Na_2CO_3) until reaching a pH of 7. It was then dried at 80°C and sieved through a 53-micrometer sieve, referred to as ACP. Samples were taken for analysis.

2.2.2. Modified to Prepare (ACPO)

After that, the resulting ACP was modified activated with 100 mL of H_2O_2 at 120°C and stirred for 24 hrs, then it was filtered and washed three times with distilled water, dried in an oven at 80°C, sieved again using a 53-micrometer sieve, and labeled as ACPO. Samples were taken for FTIR, XRD, FESEM, TEM, and EDX analyses, and it was found that the activated charcoal (ACPO) is nanoscale charcoal, so it was selected for the next experiment.

2.3. Preparation of Adsorbates

A series of solutions was prepared with a volume of 100 mL at concentrations of 20000, 40000, 60000, 80000, and 100000 ppm by diluting 2g, 4g, 6g, 8g, and 10g in 100 mL of distilled water for concentrated Citric acid.

2.4. Batch Adsorption Studies

The tests were conducted in sealed containers 50 mL polyethylene containers. A weighed amount (0.1 g) of the adsorbent material was added to the solution, and using a rotary shaker, the initial concentrations (20000,40000,60000,80000,and 100000 ppm), contact times (15, 30, 45, 60, 75, 90, 105, 120, 180, and 240 minutes), adsorbent doses (0.1, 0.3, 0.5, 0.7, 1 g), and temperature variations (25, 35, 45, and 55°C). The amount of Citric acid retained, in mg per gram, was determined using a mass balance equation (1).[29]

$$Qe = \frac{Co-Ce}{m} \times V \qquad (1)$$

Where Co is the initial concentration of acid in ppm, Ce is the equilibrium acid concentration in ppm, Qe is

the amount of acid adsorbed onto per unit weight of the adsorbent in mg/g, V is the volume of adsorbate in liter and m is the weight of the adsorbent in grams. The percentage of removal

of acid was calculated from the following equation (2).[30]

$$Removal(\%) = \frac{Co-Ce}{Co} \times 100 \qquad (2)$$

3. Result and Discussion:

3.1. Characterization on Functions Surface

3.1.1. FTIR ANALYSIS

3.1.1.1. FTIR Analysis OF ACP

The FTIR spectrum as show in **Figure.1** showed O-H stretching broad at 3671 and 3686 cm^{-1} corresponding to the phenol group, and an O-H stretching band at 3231 cm^{-1} indicating the presence of a hydrogen-bonded O-H group. Three bands appear for CH2 and CH3 stretching: the first and second at 2987 and 2972 cm^{-1} correspond to symmetric vibrations, and the third at 2901 cm^{-1} corresponds to asymmetric vibrations. A band at 2573 cm^{-1} indicates O-H stretching, and a band at 2361 cm^{-1} indicates CO2 absorption. Bands at 2163 and 2191 cm^{-1} correspond to overtone bands of aromatic C=C. Bands at 1539 and 1556 cm^{-1} correspond to aromatic C=C stretching, a band at 1407 cm^{-1} corresponds to C-H bending, and bands at 1228, 1250, 1055, 1066, and 1075 cm^{-1} correspond to C-O stretching of phenols, alcohols, or ethers. A band at 874 cm^{-1} corresponds to out-of-plane bending of aromatic C-H. Bands at 565, 593, and 611 cm^{-1} correspond to C-X stretching, and Bands at 517, 536, and 553 cm^{-1} correspond to ring skeletal vibrations.

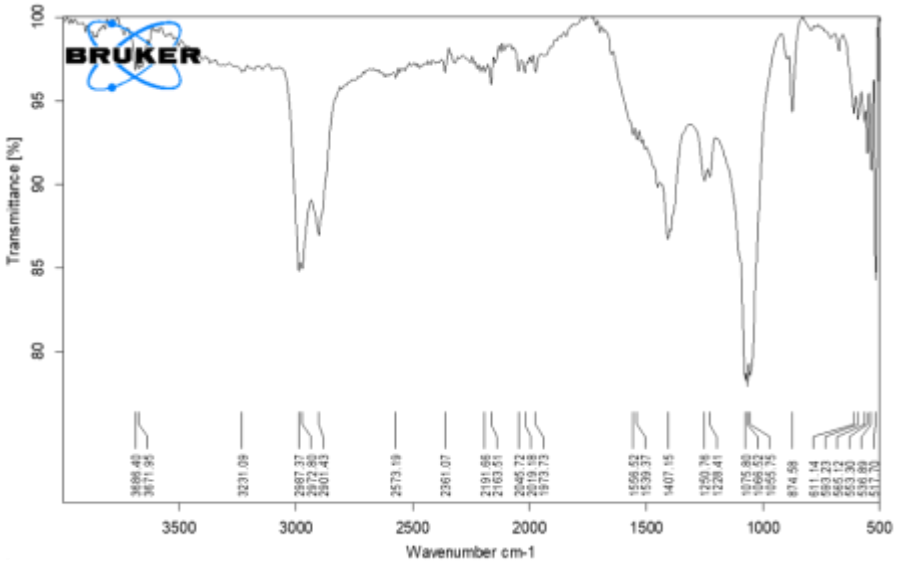

Figure 1: FT-IR Spectrum of ACP

3.1.1.2 FTIR Analysis OF modified-ACPO

The FTIR spectrum of modified-ACPO as show in **Figure.2** showed O-H stretching broad at 3665 and 3686, belonging to the phenol group, and three bands: the first and second at 2987 and 2973 correspond to symmetric vibrations, while the third band at 2901 corresponds to asymmetric vibrations. These bands are attributed to CH2 and CH3 stretching. A band at 2326 indicates CO2 absorption. Peaks at 1573 and 1554 correspond to aromatic C=C, peaks at 1451 to C-H bending, and bands at 1227, 1249, 1050, 1066, 1075 correspond to C-O stretching associated with phenols, alcohols, or ethers. A band at 879 corresponds to aromatic C-H out-of-plane bending, and bands at 637 and 515 correspond to ring skeletal vibrations. Bands at 1680 and 1694 correspond to C=O stretching, and bands at 1393 and 1406 correspond to O-H bending.

Table.1 shows the peaks of ACP and ACPO, allowing for a comparison between the peaks present in each of them.

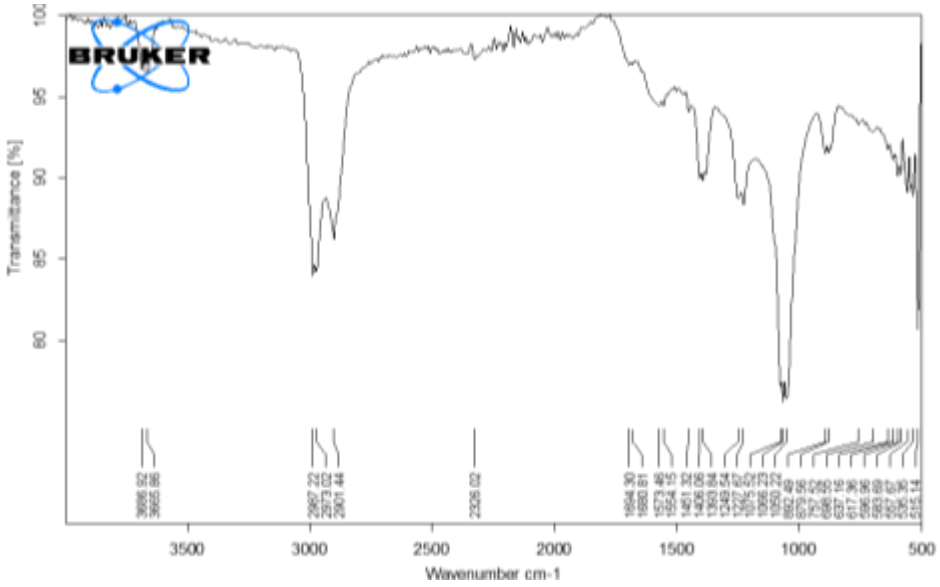

Figure 2: FT-IR Spectrum OF modified-ACPO

Table.1 shows the Peaks of ACP and ACPO

ACPO Wavenumber (cm^{-1})	ACP Wavenumber (cm^{-1})	Type of bond
3665,3686	3686 ,3671	Stretching O–H
Not available	3231	Linked by hydrogen bonds O–H
2987,2973,2901	2987,2972,2901	Stretching C–H
Not available	2573	Acidity O-H
2326	2361	Absorption CO_2
Not available	2163,2191	Overtone bands of aromatic C=C
1554,1573	1539,1556	aromatic C=C
1451	1407	Bending C-H
1249,1227	1250,1228	Stretching C–O
1050,1066,1075	1055,1066,1075	Strong Stretching C–O
879	874	Out-of-plane bending C–H
515,637	517,536,553	Structural vibrations of the ring
Not available	565,593,611	C-X
1680,1694	Not available	Stretching C=O
1393,1406	Not available	Bending O-H

3.1.2.(XRD) Analysis

3.1.2.1 XRD Analysis OF ACP

The X-ray diffraction (XRD) pattern of ACP powder shown in **Figure.3** and data peaks in **Tabel.2** for carbon before the activation stage shows strong and weak diffraction peaks at 2θ = 23°, 2θ = 25°, 2θ = 29°, 2θ = 31°, 2θ = 41°and 2θ = 43°, respectively. The average crystal size of ACP carbon is 14.23 nm.

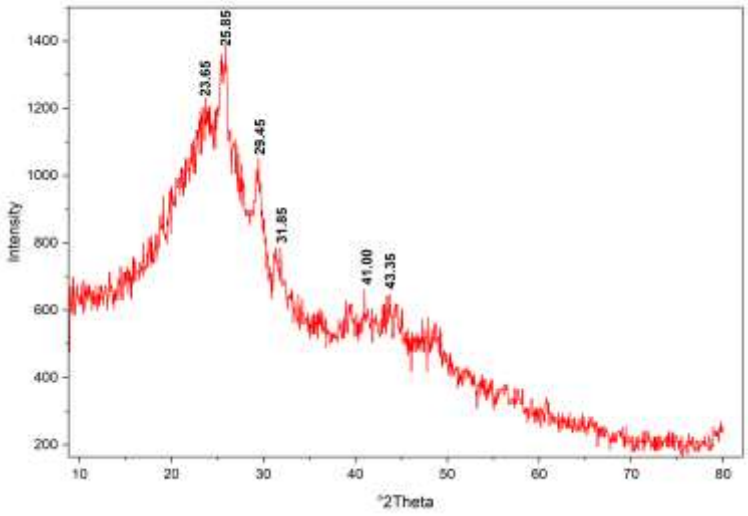

Figure 3. XRD for ACP

Table. 2 Data for the four strongest peaks in the X-ray diffraction spectrum of carbon ACP

Miller indices (hkl)	2θ (degree)	FWHM (degree)	Crystallite size D (nm)
221	23.65	0.20	38.86
331	25.85	0.30	25.79
400	29.45	1.16	6.62
401	31.85	7.00	1.09
223	41.15	0.60	12.39
530	43.35	11.02	0.66
Average crystalline size D			14.23 nm

3.1.2.2 XRD Analysis OF ACPO

X-ray diffraction (XRD) pattern of ACPO powder for activated carbon produced by chemical activation using H_2O_2 (after the washing stage) shows diffraction peaks at 2θ = 14°, 2θ = 24°, 2θ = 26°, 2θ = 44°, 2θ = 48°and 2θ = 62°, respectively. The average crystallite size in ACPO activated carbon is 7.34 nm. shown in the **Figure.4** and data peaks in **Tabel.3**

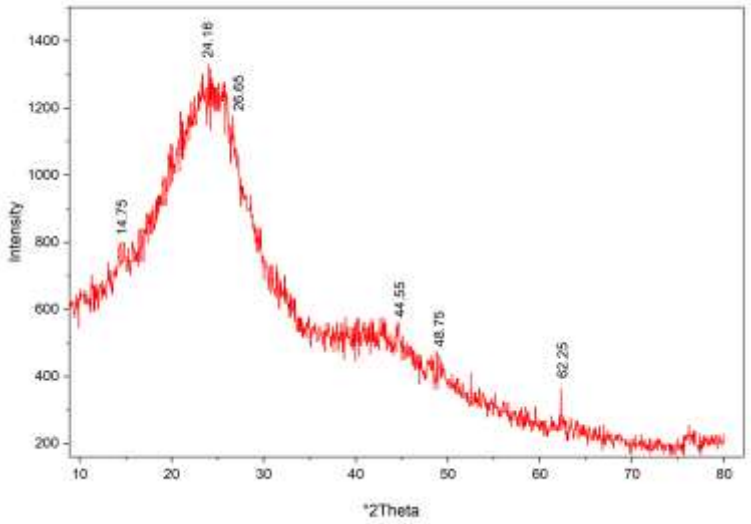

Figure 4. XRD for modified-ACPO

Tabel.3 Data for the four strongest peaks in the X-ray diffraction spectrum of carbon ACPO

Miller indices (hkl)	2θ (degree)	FWHM (degree)	Crystallite size D (nm)
102	**14.75**	**0.20**	**39.37**
311	**24.16**	**7.09**	**1.09**
313	**26.65**	**5.30**	**1.45**
610	**44.55**	**10.84**	**0.67**
194	**48.75**	**11.60**	**0.62**
393	**62.25**	**7.80**	**0.87**
Average crystalline size D			**7.34 nm**

3.1.3. SEM Analysis

3.1.3.1. SEM Analysis OF ACP

The (SEM) image of ACP shown in **Figure.5** reveals an irregular surface structure with a scaly and cracked appearance, containing particles of different sizes and heterogeneous clusters. This is due to the collapse of the original plant structure and the formation of a fragile carbonaceous material.[31][32].

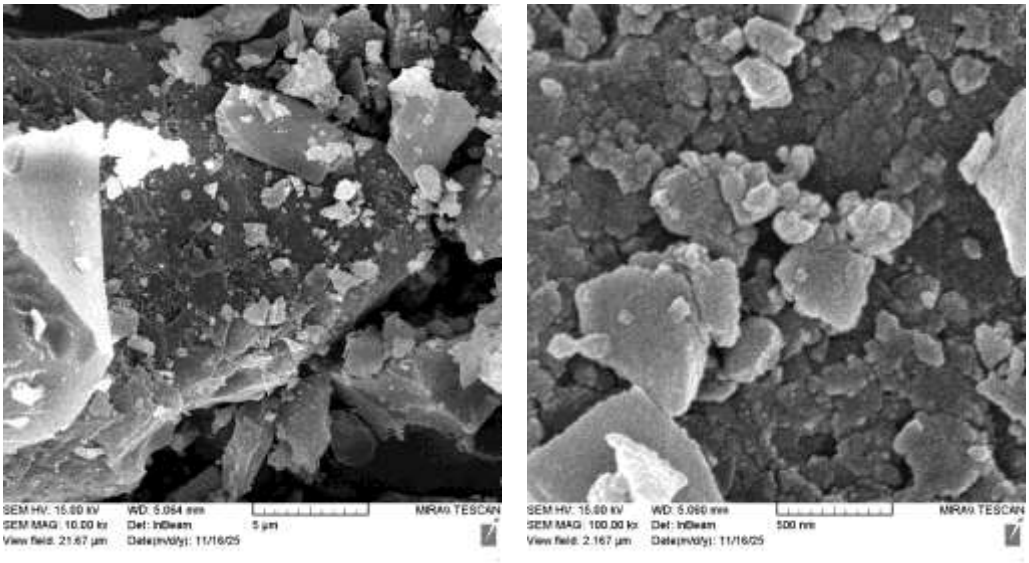

Figure 5. SEM for ACP

3.1.3.2. SEM Analysis OF modified - ACPO

The (SEM) image of modified-ACPO shown in **Figure.6** shows an irregular and rough surface structure, composed of carbon aggregates with flaky and fragmented shapes, with a clear gradient in particle sizes and partial agglomeration among them. A significant presence of voids and surface cracks is observed, along with irregular cavities, indicating effective chemical etching during the activation process. Activation with peroxide caused the carbon structure to break down and opened closed pores, which contributed to an increase in the effective surface area and improved the adsorption properties of the charcoal[31], [32].

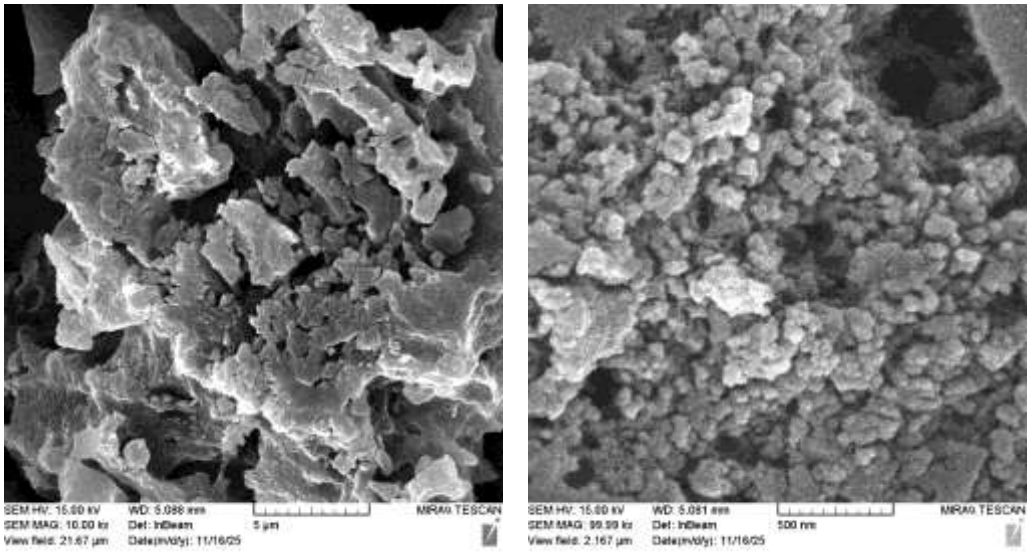

Figure 6. SEM for modified-ACPO

3.1.4. EDX Analysis OF ACP and modified - ACPO

EDX technology analyzes the elements in the activated carbon sample as shown in **Figure.7 And Figure.8 ,Tabel.4 and Tabel.5** The carbon peak can be seen in the EDX spectrum, and other impurities can be observed.

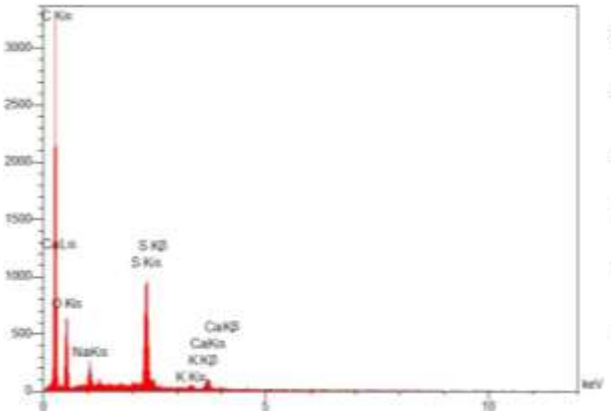

Figure 7. EDX for ACP

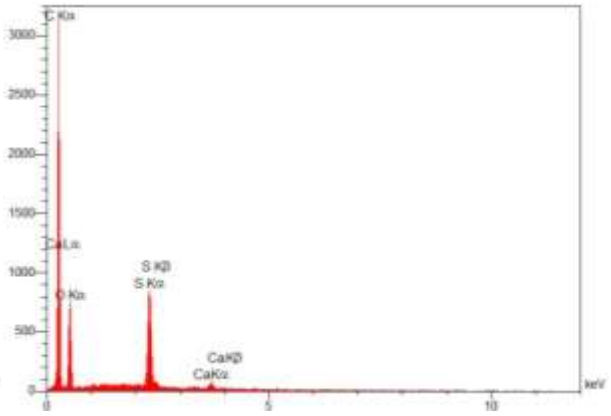

Figure 8. EDX for modified-ACPO

Tabel 4. EDX for ACP

Elt	W%	A%
C	60.37	73.48
O	17.51	16.00
Na	3.82	2.43
S	15.50	7.07
K	0.83	0.31
Ca	1.98	0.72
	100.00	100.00

Tabel 5. EDX for modified-ACPO

Elt	W%	A%
C	63.44	74.67
O	21.03	18.58
S	14.48	6.38
Ca	1.06	0.37
	100.00	100.00

3.1.5. TEM Analysis

3.1.5.1. TEM Analysis OF ACP

The (TEM) images of ACP shown in **Figure.9** reveal an aggregated nanostructure composed of semi-spherical and irregularly shaped carbon particles, with sizes within the nanoscale range. A clear contrast in shades is observed, indicating a heterogeneous density distribution and the presence of internal nanopores. The absence of regular crystalline patterns also indicates the amorphous nature of the charcoal. This porous nanostructure contributes to an increased surface area and enhances the adsorption properties of the charcoal[33]

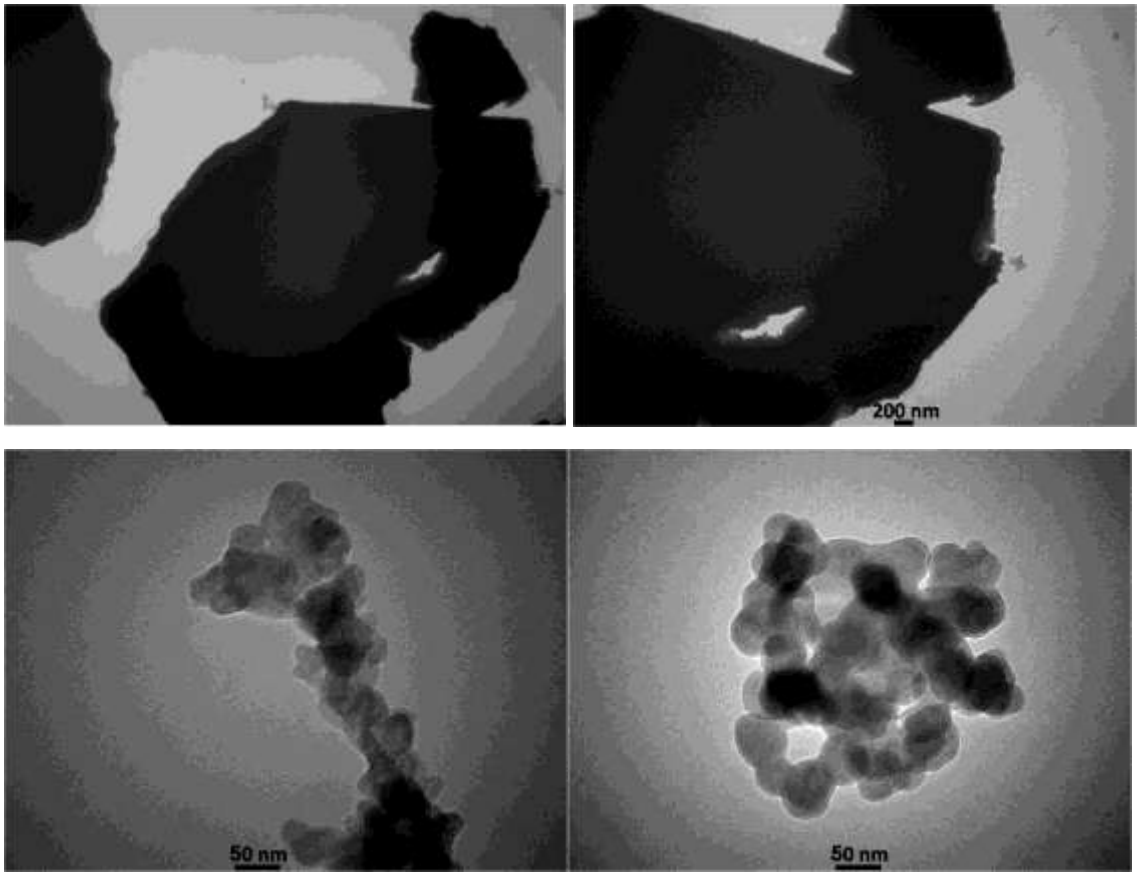

Figure 9.TEM for ACP

3.1.5.2 TEM Analysis OF modified-ACPO

Microscopic examination reveals the presence of irregularly shaped spherical carbon nanoparticles that tend to form clusters or branched chains. This aggregation reflects the nature of surface interactions during the chemical activation process. [33]as shown in the **Figure.10**

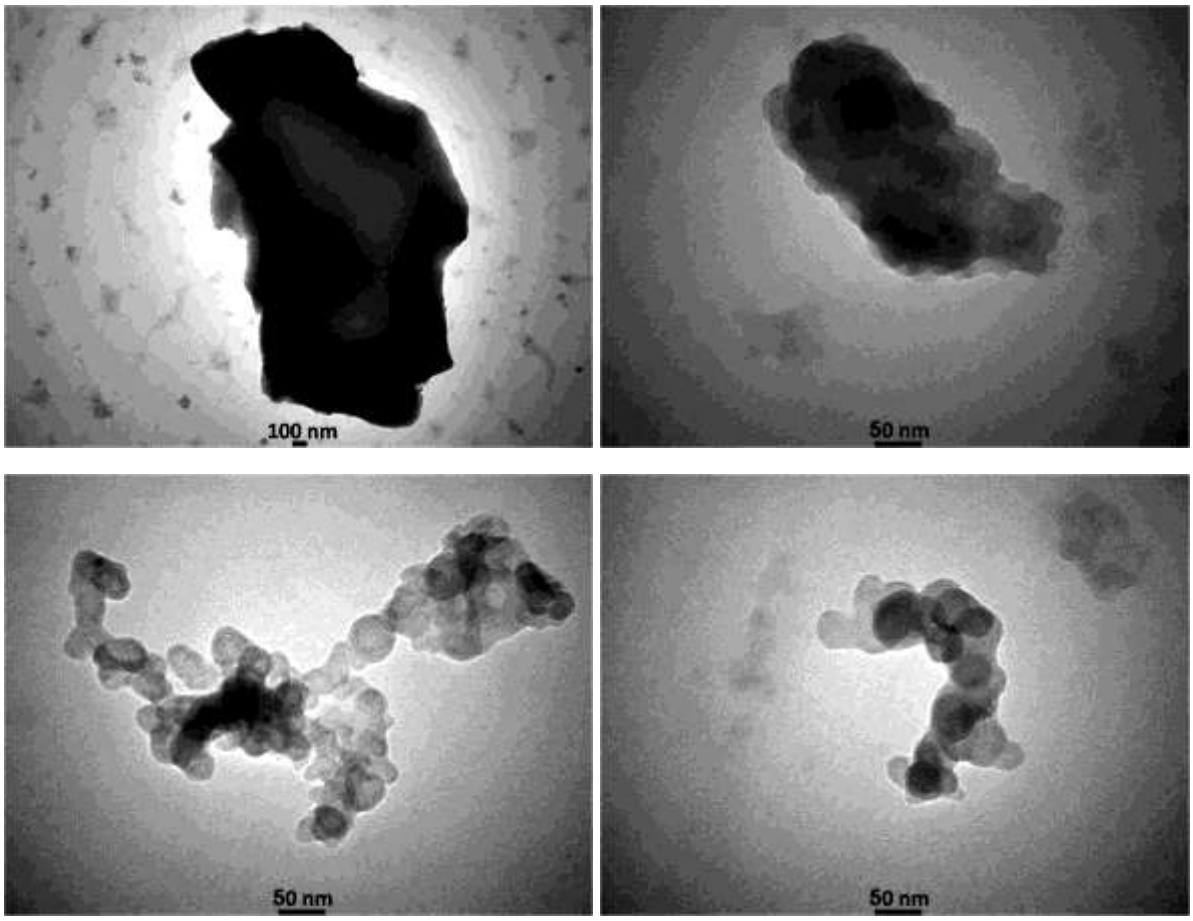

Figure.10 TEM for ACPO

3.1.6. AFM Analysis

3.1.6.1. AFM Analysis OF ACP

The (AFM) images of the biochar surface topography showed an irregular structure

with high surface roughness, with significant variations in height within the nanoscale range, and a height range of approximately 262 nm. This variation indicates the presence of nanoscale protrusions and depressions evenly distributed across the surface, as shown in the **Figure.11 and Figure.12.**

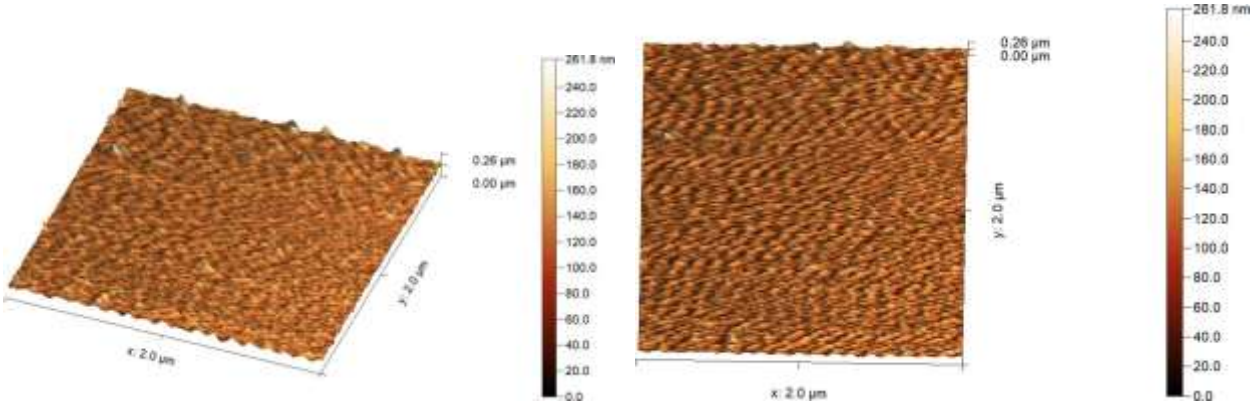

Figure 11. AFM of ACP

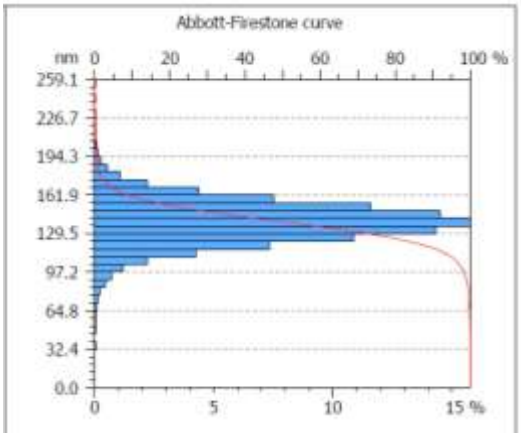

Figure 12. Percentage of ACP sizes

3.1.6.2. AFM Analysis OF modified-ACPO

AFM images show two- and three-dimensional shapes of the biochar surface topography, with an irregular structure and noticeable surface roughness, with a height range of about 160 nm as shown in the **Figure.13 and Figure.14.**

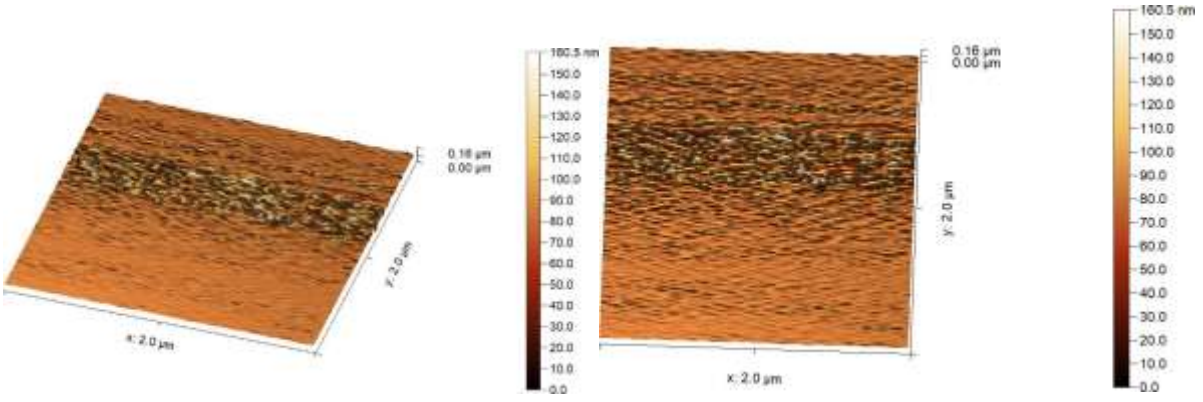

Figure 13. AFM of modified-ACPO

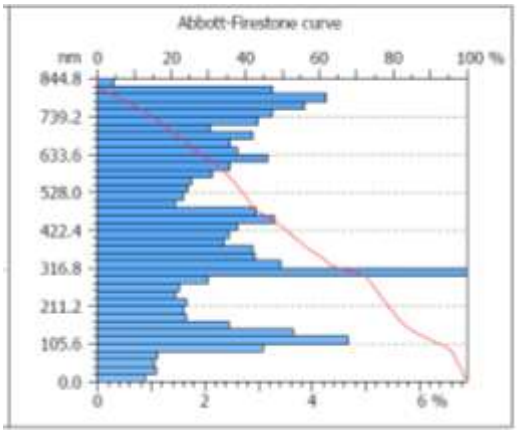

Figure 14. Percentage of modified-ACPO sizes

3.2. study of Effect the Operational Parameters

Adsorption is influenced by numerous factors, including the initial acid concentration, the amount of adsorbent, temperature, nature of the adsorbent, and the contact time.

3.2.1. Effect of Initial Concentration

The initial acid concentration is one of the main factors affecting the equilibrium concentration. **Figure 15**. illustrates the effect of Citric acid concentration on ACPO. The acid R % decreased as a result of the high initial acid concentration.[34]

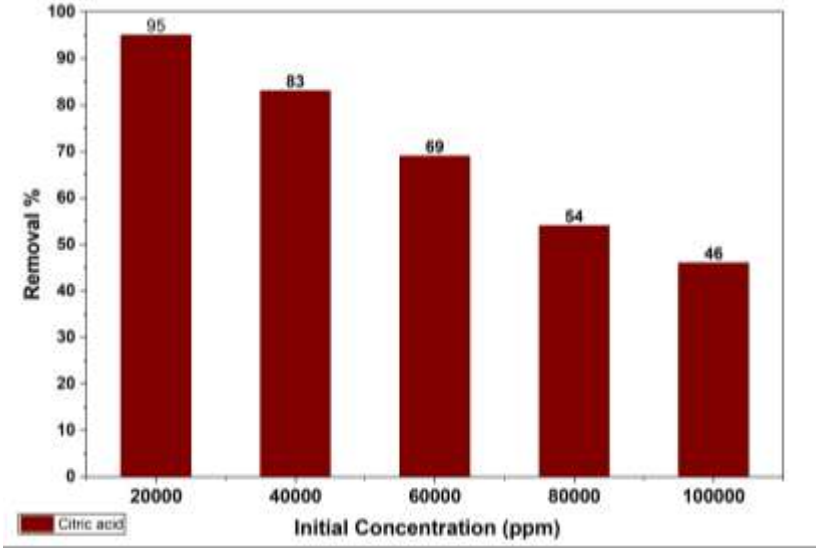

Figure 15. shows the R% of Citric acid at different concentration of modified ACPO

3.2.2. Effect of Temperature

Temperature is one of the factors affecting the absorption process [35]. The effect of temperature on the absorption of Citric acid was investigated using different temperatures ranging from 25, 35, 45, to 55 C^{o}. The removal percentage of Citric acid at 25°C was 78%, while the highest removal rate occurred at 55°C was 96%, as shown in the **Figure.16.**

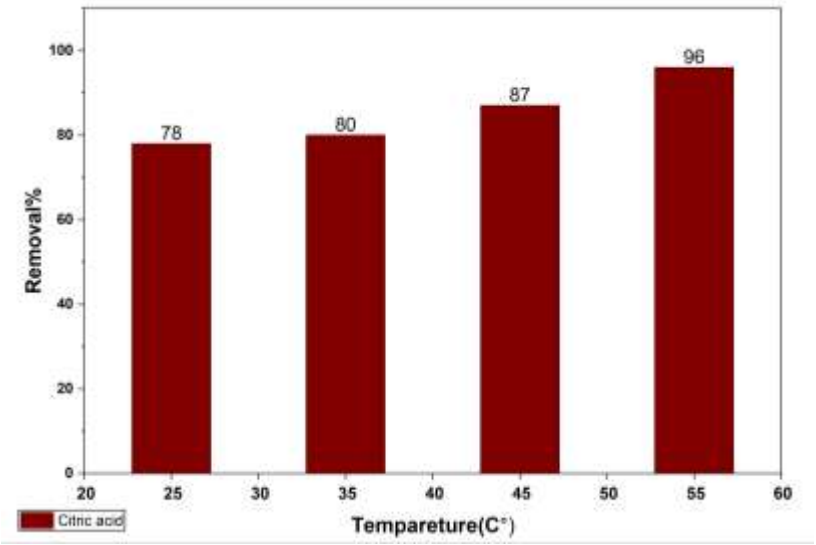

Figure 16. Shows the R% of Citric acid at different temperatures of modified ACPO

3.2.3. Influence of Adsorbent Dose on Adsorption

Another important variable in improving the absorption system is the adsorbent dose[36]. Using different doses of activated charcoal ranging from 0.1 to 1 gram, the effect of the adsorbent dose on Citric acid absorption was studied. **Figure 17** shows how the amount of adsorbent increases with the removal of Citric acid. 83% of Citric acid was removed when using 0.1 grams of activated charcoal. The removal efficiency tended to increase, reaching 98% when the dose was increased to 1 gram. The increase in absorption with a higher adsorbent dose may be due to the larger surface area and the availability of more sites on the adsorbent surface[36].

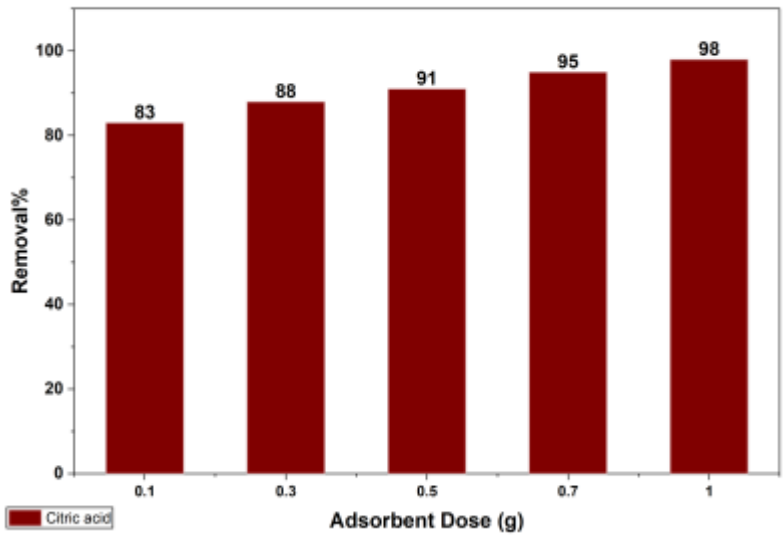

Figure 17. Shows the R% of Citric acid at different adsorbent dose of ACPO.

3.2.4. Influence of Contact Time on Adsorption

In addition, batch adsorption studies were conducted at different contact times (15, 30, 45, 60, 75, 90, 105, 120, 180, and 240 minutes) using an initial concentration of 2% Citric acid with 0.1 grams of activated charcoal as the adsorbent in 50 mL of Citric acid solution at 25°C. **Figure 18** illustrates the effect of contact time on Citric acid removal by activated charcoal. This is essential for the adsorption process because the contact time between the adsorbent and the substance depends on the type of system used. These graphs show how quickly the acid is absorbed initially, but eventually, it slows down and reaches equilibrium[36].

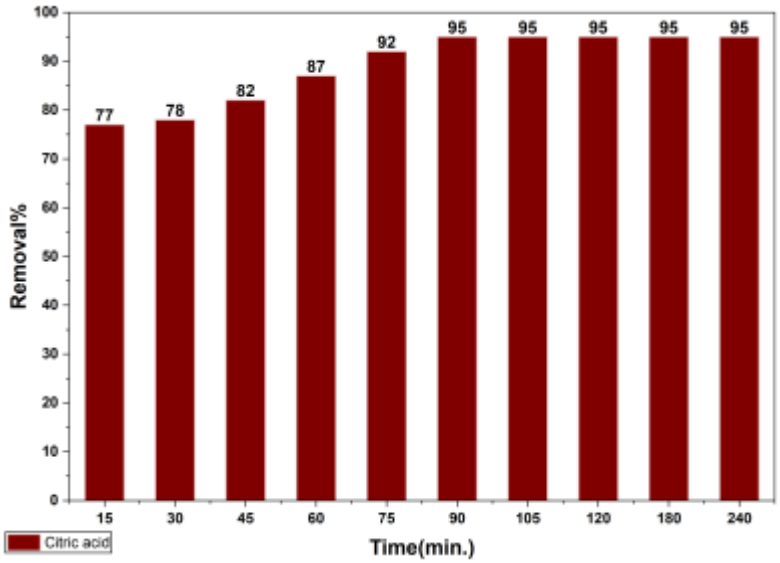

Figure 18. Shows the R% of Citric acid at different the time on ACPO

3.3. Adsorption Isotherm

3.3.1. Isothermal Langmuir adsorption

The results of the Langmuir model for the removal of Citric acid from activated carbon are shown in **Figure 19**. The correlation coefficients provided strong evidence for the adsorption of Citric acid on activated carbon after isothermal Langmuir. The linear application of the Langmuir model to activated carbon showed excellent correlation coefficients R. For Citric acid, R2 = 0.9587. This indicates that the Langmuir curve provides a reasonable representation of the adsorption system[37]

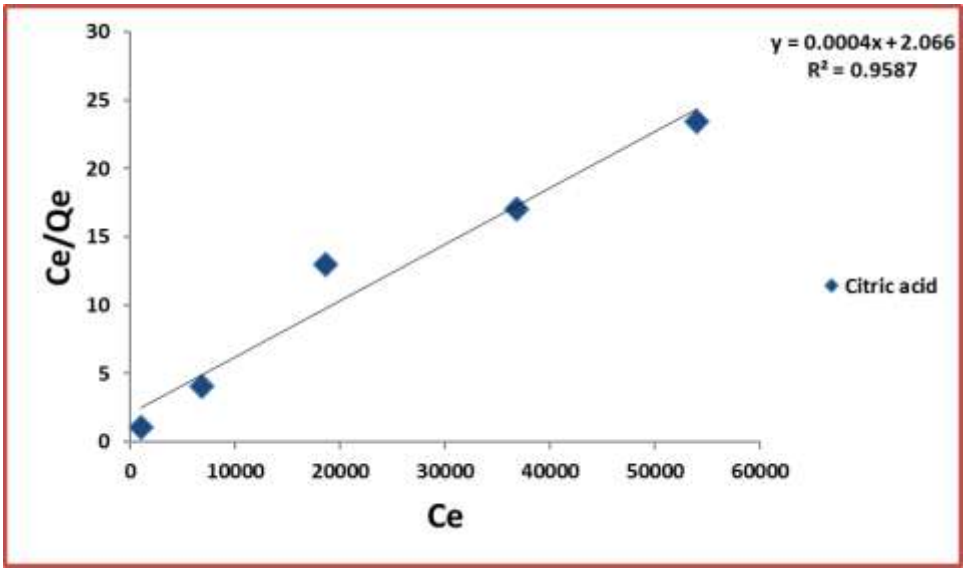

Figure 19. Shows the Langmuir isotherm for the adsorption of Citric acid on modified ACPO

3.3.2. Freundlich Isotherm Adsorption

The value of the Freundlich adsorption constant, 1/n, is greater than one, as shown by **Figure 20**. and **Table 6.** The application of the linear form of the Freundlich model to modified ACPO was shown by the high correlation coefficients R. For Citric acid, R2 = 0.9714. This implies that an appropriate model of the adsorption system is provided by the Freundlich isotherm[38]The Freundlich isotherm model exhibited a higher correlation coefficient than the Langmuir model and indicates better agreement with the experimental adsorption data. This suggests that adsorption occurred on a heterogeneous surface with a non-uniform energy distribution, which is characteristic of activated carbon materials. Therefore, the Freundlich model describes the adsorption behavior of modified-ACPO more precisely.

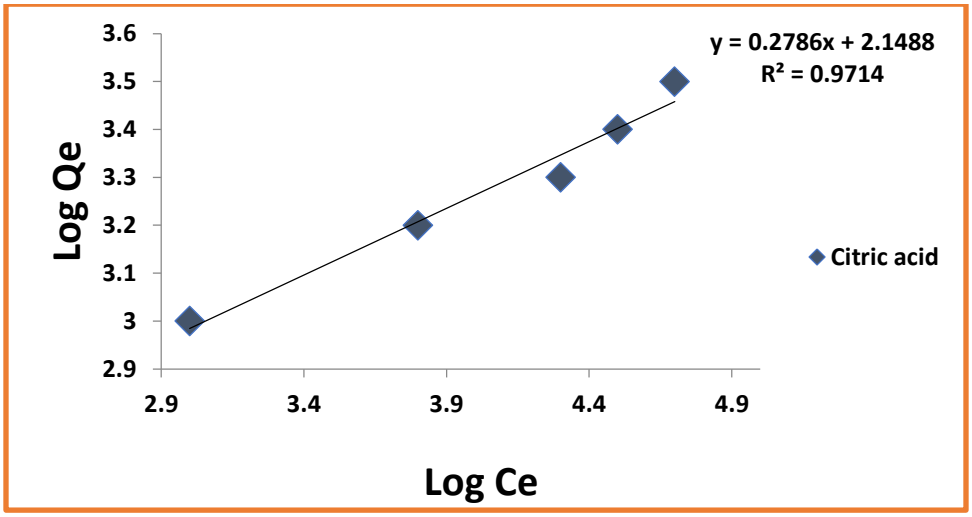

Figure 20. Shows the Freundlich isotherm for the adsorption of Citric acid on modified ACPO.

Table 6. Shows the Langmuir and Freundlich constants for the adsorption of Citric acid.

Adsorbent	Langmuir constants			Freundlich constants		
	R^2	$Q_{o\ max}$	K_L	R^2	n	k_f
Citric acid	0.9587	2500	1.94×10^{-4}	0.9714	3.59	141

3.4. Thermodynamic Study

Carbon activated with hydrogen peroxide was used to determine the thermodynamic functions of the adsorption processes (Citric acid) from aqueous solutions. The Vant Hoff equation was utilized to get the enthalpy of adsorption (ΔH) and entropy of adsorption (ΔS) values[39].

$$LnK=\Delta S/R-\Delta H/RT,\quad K=Qe/Ce \qquad (4)$$

The straight-line equation's slope and intercept were found by plotting Ln K vs 1/T in **figures 21.** From the equation's slope and intercept, respectively, ΔH and ΔS values were obtained. The Kipps mathematical equation was also used to calculate the value of the free energy ΔG[40]

$$\Delta G=\Delta H-T\cdot\Delta S \qquad (5)$$

Since the heat of absorption (ΔH) is negative for Citric acid and its value is less than 40 kJ/mol, as shown in **Table 7.** this means that the absorption process releases heat accompanied by a decrease in entropy. The negative values of ΔG indicate spontaneous absorption activity, which increases with rising temperature. The negative value of ΔS indicates that the molecular ordering on the surface is higher than in the solution.

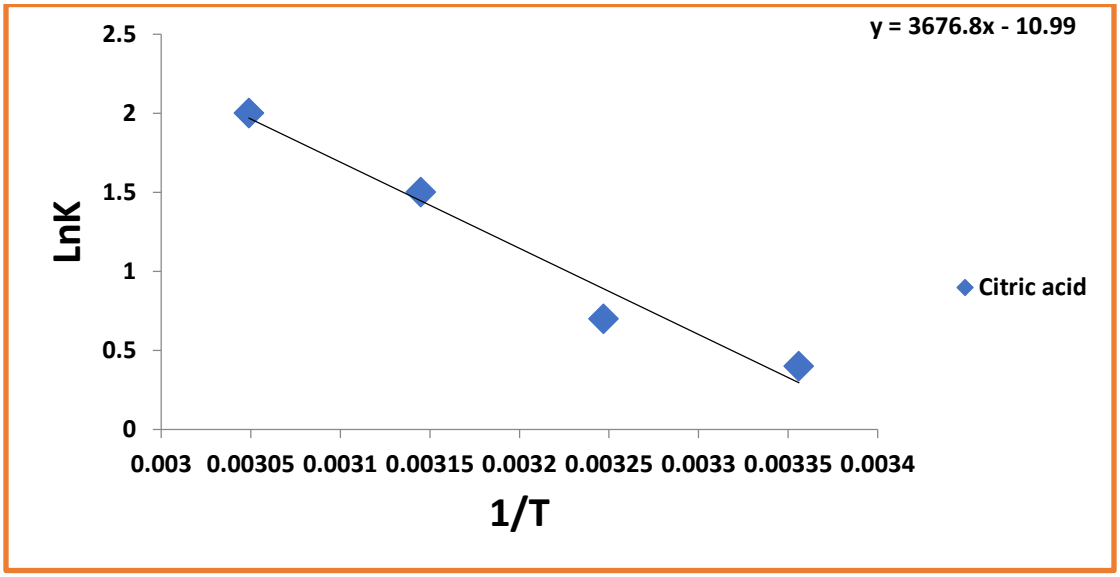

Figure 21. Van't Hoff relationship for the removal of Citric acid on modified-ACPO.

Table 7. Shows the thermodynamic values for Citric acid.

T(K)	Citric acid		
	ΔH (KJ/mol)	**ΔG (KJ/mol)**	**ΔS (KJ/mol.)**
298	-30.6	-1.41	-91.4
308		-1.77	
318		-3.20	
328		-6.78	

Conclusions:

Modified-activated carbon ACPO was prepared using pomegranate peels, and hydrogen peroxide treatment was applied to enhance the carbon's adsorption efficiency. Its properties were studied using EDX, FE-SEM, XRD, TEM, and AFM techniques. The Citric acid removal percentage was calculated; it was found that the Citric acid removal percentage was 95%. Additionally, the amount of acid adsorbed increased with increasing contact time. Freundlich and Langmuir equations were applied to the adsorption process the results showed a better fit with the Freundlich model, and thermodynamic functions were calculated, yielding ΔH = -30.6 and ΔS = -91.4 for Citric acid.

References

[1] K. E. Murray, S. M. Thomas, and A. A. Bodour, "Prioritizing research for trace pollutants and emerging contaminants in the freshwater environment," Dec. 2010. doi: 10.1016/j.envpol.2010.08.009.

[2] M. T. García-Córcoles *et al.*, "Chromatographic Methods for the Determination of Emerging Contaminants in Natural Water and Wastewater Samples: A Review," Mar. 04, 2019, *Taylor and Francis Ltd.* doi: 10.1080/10408347.2018.1496010.

[3] H. Foya, J. E. G. Mdoe, and L. L. Mkayula, "Adsorption of Maleic and Oxalic Acids on Activated Carbons Prepared from Tamarind Seeds." [Online]. Available: www.ijert.org

[4] P. G. Blower, E. Shamay, L. Kringle, S. T. Ota, and G. L. Richmond, "Surface behavior of malonic acid adsorption at the air/water interface," *Journal of Physical Chemistry A*, vol. 117, no. 12, pp. 2529–2542, Mar. 2013, doi: 10.1021/jp310851j.

[5] A. Berhe, A. Jeevan, and T. Lijalem, "Removal of Acetic Acid from Aqueous Solution by using Activated Carbon," 2015. [Online]. Available: http://www.ijisr.issr-journals.org/

[6] Worch and Eckhard, "Eckhard Worch Adsorption Technology in Water Treatment."

[7] B. Duruaku Jacinta Nkiruka, "MODIFICATION OF SURFACE, PHYSICAL AND CHEMICAL PROPERTIES OF ACTIVATED CARBONS FOR WATER PURIFICATION," 2012.

[8] M. P. C, "Physicochemical characteristics of activated charcoal derived from melon seed husk," *Available online www.jocpr.com Journal of Chemical and Pharmaceutical Research*, vol. 5, no. 5, pp. 94–98, 2013, [Online]. Available: www.jocpr.com

[9] D. Egirani, M. T. Latif, N. Wessey, N. R. Poyi, and N. Shehata, "Preparation and characterization of powdered and granular activated carbon from Palmae biomass for mercury removal," *Appl. Water Sci.*, vol. 11, no. 1, Jan. 2021, doi: 10.1007/s13201-020-01343-8.

[10] M. J. Ahmed and S. K. Theydan, "Physical and chemical characteristics of activated carbon prepared by pyrolysis of chemically treated date stones and its ability to adsorb organics," *Powder Technol.*, vol. 229, pp. 237–245, Oct. 2012, doi: 10.1016/j.powtec.2012.06.043.

[11] L. Sellaoui *et al.*, "Adsorption of emerging pollutants on lignin-based activated carbon: Analysis of adsorption mechanism via characterization, kinetics and equilibrium studies," *Chemical Engineering Journal*, vol. 452, Jan. 2023, doi: 10.1016/j.cej.2022.139399.

[12] M. N. Ettish, G. S. El-Sayyad, M. A. Elsayed, and O. Abuzalat, "Preparation and characterization of new adsorbent from Cinnamon waste by physical activation for removal of Chlorpyrifos," *Environmental Challenges*, vol. 5, Dec. 2021, doi: 10.1016/j.envc.2021.100208.

[13] Z. Heidarinejad, M. H. Dehghani, M. Heidari, G. Javedan, I. Ali, and M. Sillanpää, "Methods for preparation and activation of activated carbon: a review," Mar. 01, 2020, *Springer Science and Business Media Deutschland GmbH*. doi: 10.1007/s10311-019-00955-0.

[14] A. T. Alves, D. J. Lasmar, I. P. de Andrade Miranda, J. da Silva Chaar, and J. dos Santos Reis, "The Potential of Activated Carbon in the Treatment of Water for Human Consumption, a Study of the State of the Art and Its Techniques Used for Its Development," *Advances in Bioscience and Biotechnology*, vol. 12, no. 06, pp. 143–153, 2021, doi: 10.4236/abb.2021.126010.

[15] S. Bubanale and M. Shivashankar, "History, Method of Production, Structure and Applications of Activated Carbon." [Online]. Available: www.ijert.org

[16] R. Nedjai, N. A. Kabbashi, M. Z. Alam, and M. F. R. Al-Khatib, "Production and Characterization of Activated Carbon from Baobab Fruit Shells by Chemical Activation Using ZnCl2, H3PO4 and KOH," in *Journal of Physics: Conference Series*, IOP Publishing Ltd, Dec. 2021. doi: 10.1088/1742-6596/2129/1/012009.

[17] S. A. A and G. W. A, "EVALUATION OF GROUNDWATER CONTAMINATION STATUS IN IGANDO AREA OF LAGOS STATE, NIGERIA."

[18] A. O. Oluwatoyin and A. A. Olalekan, "Adsorption of Crude Oil Spill from Aqueous Solution using Agro-Wastes as Adsorbents," *J. Sci. Res. Rep.*, pp. 27–52, May 2021, doi: 10.9734/jsrr/2021/v27i430376.

[19] F. Barjasteh-Askari, M. Davoudi, M. Dolatabadi, and S. Ahmadzadeh, "Iron-modified activated carbon derived from agro-waste for enhanced dye removal from aqueous solutions," *Heliyon*, vol. 7, no. 6, Jun. 2021, doi: 10.1016/j.heliyon.2021.e07191.

[20] J. B. Njewa, E. Vunain, and T. Biswick, "Synthesis and Characterization of Activated Carbons Prepared from Agro-Wastes by Chemical Activation," *J. Chem.*, vol. 2022, 2022, doi: 10.1155/2022/9975444.

[21] I. Neme, G. Gonfa, and C. Masi, "Preparation and characterization of activated carbon from castor seed hull by chemical activation with H3PO4," *Results in Materials*, vol. 15, Sep. 2022, doi: 10.1016/j.rinma.2022.100304.

[22] N. U. Udeh and V. E. Amah, "Modelling the Adsorption of Lead (II) Ion from Aqueous Phase with Carica papaya Trunk Activated Carbon," *Journal of Engineering Research and Reports*, pp. 44–54, May 2022, doi: 10.9734/jerr/2022/v22i817553.

[23] N. Abderrahim, I. Boumnijel, H. Ben Amor, and R. Djellabi, "Heat and ZnCl2 chemical carbonization of date stone as an adsorbent: optimization of material fabrication parameters and adsorption studies," *Environmental Science and Pollution Research*, vol. 29, no. 30, pp. 46038–46048, Jun. 2022, doi: 10.1007/s11356-022-19132-y.

[24] E. O. Ohimor, D. O. Temisa, and P. I. Ononiwu, "Production of Activated Carbon from Carbonaceous Agricultural Waste Material: Coconut Fibres," *Nigerian Journal of Technology*, vol. 40, no. 1, pp. 19–24, Mar. 2021, doi: 10.4314/njt.v40i1.4.

[25] Shaba, Mathew, M. Musah, M. Mohammed, A. I. Muhammad, and H. C. Obetta, "ADSORPTION OF HEAVY METALS FROM ELECTROPLATING WASTEWATER USING GUINEA CORN HUSK ACTIVATED CARBON," 2021.

[26] "Igbemi, Igbemi & Nwaogazie, Ify & Akaranta, Onyewuchi & Abu, Gideon. (2021). Adsorption Dynamics of Agricultural Waste Activated Carbon in Water Quality Improvement. European Journal of Engineering and Technology Research. 6".

[27] F. Islam *et al.*, "Functional and Nutraceutical Properties of Protein and Polyphenols Extracted From Agro-Industrial Waste: A Comprehensive Review," Feb. 01, 2026, *John Wiley and Sons Inc*. doi: 10.1002/efd2.70107.

[28] S. Ben-Ali, "Application of Raw and Modified Pomegranate Peel for Wastewater Treatment: A Literature Overview and Analysis," 2021, *Hindawi Limited*. doi: 10.1155/2021/8840907.

[29] S. S. Tahir and N. Rauf, "Removal of a cationic dye from aqueous solutions by adsorption onto bentonite clay," *Chemosphere*, vol. 63, no. 11, pp.

1842–1848, 2006, doi: 10.1016/j.chemosphere.2005.10.033.

[30] D. MOHAMMADYANI, S. A. HOSSEINI, and S. K. SADRNEZHAAD, "CHARACTERIZATION OF NICKEL OXIDE NANOPARTICLES SYNTHESIZED VIA RAPID MICROWAVE-ASSISTED ROUTE," *Int. J. Mod. Phys. Conf. Ser.*, vol. 05, pp. 270–276, Jan. 2012, doi: 10.1142/s2010194512002127.

[31] S. Henning and R. Adhikari, "Scanning Electron Microscopy, ESEM, and X-ray Microanalysis," in *Microscopy Methods in Nanomaterials Characterization*, Elsevier, 2017, pp. 1–30. doi: 10.1016/B978-0-323-46141-2.00001-8.

[32] K. S. Sim, I. Bukhori, D. C. Y. Ong, and K. B. Gan, "Signal-to-Noise Ratio in Scanning Electron Microscopy: A Comprehensive Review," 2025, *Institute of Electrical and Electronics Engineers Inc.* doi: 10.1109/ACCESS.2025.3603013.

[33] R. F. Egerton, "Physical Principles of Electron Microscopy."

[34] T. Mahroos Searan, M. Muhammed Sirhan, and H. H. Hussein, "Removal of Succinic and Phthalic Acid from Aqueous Solutions Using Activated Charcoal Prepared from the Desert Plant," *Iraqi Journal of Desert Studies*, vol. 2024, no. 2, pp. 11–25, doi: 10.36531/ijds.2024.149153.1073.

[35] "M. Jayarajan, R. Arunachalam and G. Annadurai, 2011. Agricultural Wastes of Jackfruit Peel Nano-Porous Adsorbent for Removal of Rhodamine Dye. Asian Journal of Applied Sciences, 4 263-270.".

[36] P. D. Pathak and S. A. Mandavgane, "Preparation and characterization of raw and carbon from banana peel by microwave activation: Application in citric acid adsorption," *J. Environ. Chem. Eng.*, vol. 3, no. 4, pp. 2435–2447, Dec. 2015, doi: 10.1016/j.jece.2015.08.023.

[37] E. Kavci, J. Erkmen, and M. S. Bingöl, "Removal of methylene blue dye from aqueous solution using citric acid modified apricot stone," *Chem. Eng. Commun.*, vol. 210, no. 2, pp. 165–180, 2023, doi: 10.1080/00986445.2021.2009812.

[38] M. Abbas and M. Trari, "Mass transfer process in the removal of Congo Red (CR) onto Natural Clay (NC): Kinetic, isotherm modeling, and thermodynamic study," *Journal of Water and Climate Change*, vol. 14, no. 8, pp. 2755–2772, Aug. 2023, doi: 10.2166/wcc.2023.103.

[39] S. E. Efan and M. M. Sirhan, "USE OF ENVIRONMENTALLY FRIENDLY MATERIALS TO REMOVE SOME POLLUTANTS FROM AQUEOUS SOLUTIONS," *Biochem. Cell. Arch*, vol. 22, no. 1, pp. 3401–3411, 2022, [Online]. Available: www.connectjournals.com/bca

[40] E. A. Hamooshy and H. H. Hussein, "Thermodynamic properties study of dissolution of 2-hydroxbenzoic acid in binary solvent (ethanol+ water) at various temperatures," *Egypt. J. Chem.*, vol. 64, no. 11, pp. 6499–6504, Nov. 2021, doi: 10.21608/ejchem.2021.78220.3829.